Journal of Power Sources, *33* (1991) 27–50

Discontinuous and continuous hardening processes in calcium and calcium–tin micro-alloyed lead: influence of 'secondary-lead' impurities

L. Bouirden, J. P. Hilger and J. Hertz*

Laboratoire de Thermodynamique Métallurgique, Université de Nancy I, URA CNRS 1108, B.P. 239, 54506 Vandoeuvre-les-Nancy Cédex (France)

Abstract

Different transformations in lead–calcium and lead–calcium–tin alloys are observed with various complementary techniques such as anisothermal microcalorimetry, optical and electronic microscopy, hardness measurements. Three alloy states are studied: as-cast, rehomogenised/water-quenched, rehomogenised/air-cooled. With binary lead–calcium alloys, three successive discontinuous transformations are observed, namely: an initial and complete discontinuous transformation with regular moving of the front of reaction; a second and incomplete discontinuous transformation (puzzle-shaped); a third and incomplete discontinuous transformation with precipitation of Pb_3Ca. The role of secondary-lead impurities is complex: Ag reduces and Bi accelerates the rate of the discontinuous reaction, while Al refines the grain size. Lead–calcium–tin are characterised by the Sn/Ca ratio. For very small values of this ratio, the hardening is similar to that of lead–calcium alloys. For high ratio values, the hardening takes place after an incubation period and proceeds via a continuous micro-precipitation of the $(PbSn)_3Ca$ compound. For intermediate ratios, the different processes are able to operate separately in sequence. Ag increases the rate of the continuous precipitation and reduces the incubation time. No significant effects are observed with Bi or Al. The kinetic laws of the different transformations are presented and values for the energy of activation are determined.

Introduction

With the increasing market for maintenance-free batteries, the need to ascertain the effect of impurities in lead alloys is becoming more important. This paper reports a new study of the ageing phenomena in lead–calcium and lead–calcium–tin alloys in order to determine the influence of the trace elements Bi, Al and Ag. In particular, the work is directed towards investigation of structural morphology and the kinetics of each transformation. Three initial states are systematically studied: (i) as-cast product (with segregation cells); (ii) rehomogenised at 310 °C and water quenched; (iii) rehomogenised at 310 °C and air-cooled.

*Author to whom correspondence should be addressed.

0378-7753/91/$3.50

TABLE 1

Chemical analysis of alloys (wt.%)

Alloy	Ca	Sn	Sn/Ca	Ag	Bi	Al
786	0.058					
793	0.093					
795	0.100					
787	0.055			0.007		
783	0.090			0.001		
788	0.092			0.0006		
777	0.066					0.085
778	0.130					0.068
765	0.044				0.0312	
794	0.070				0.0320	
796	0.098				0.0320	
751	0.097				0.0370	0.002
748	0.120	0.24	0.67			
776	0.120	0.44	1.24			
779	0.110	0.64	1.96			
780	0.110	1.09	3.35			
766	0.059	0.58	3.32			
767	0.050	0.66	5.94			
771	0.069	0.88	3.23			
790	0.087	0.97	3.85	0.0006		
781	0.080	1.11	4.39	0.0027		
749	0.115	0.20	0.59			0.030
782	0.110	1.09	3.31			0.047
792	0.080	0.93	3.93		0.0600	

Experimental

Alloy composition

Table 1 summarises the composition of the various alloys under investigation. All the alloys were synthesised by dissolution of Ca, Sn, Bi, Ag or Al in a bath of pure liquid lead. The alloys were kept in liquid nitrogen after solidification and cooled at a controlled rate of 40 °C s^{-1}. Others samples were rehomogenised for 1 h at 310 °C and then quenched in water or air-cooled.

Microcalorimetry

Barberi-type calorimeters were used with linear temperature programming at a rate of 0.5 °C min^{-1} over the temperature range −10 to 110 °C, and a rate of 1 °C min^{-1} over the range 50 to 300 °C. The sample was kept under argon. Thermograms were obtained from the difference between the registered calorimetric signals during the course of two successive increments of temperature. The second heating in the calorimeter was carried out under equilibrium conditions for the alloys and served as a base-line. The sample

weight was between 5 and 15 g and the detection of the calorimeter was of the order of 10 μW.

Hardness

Vickers hardness tests were carried out on a Testwell durometer under a load of 2 kg. Each reported value of hardness corresponds to the mean of six points distributed over the whole planar surface of a given sample.

Optical microscopy

The structure of PbCa alloys undergoes progressive changes at room temperature. An optical microscopic study of the early stages of this ageing has not been accomplished previously because the time required for sample preparation is too long. Our method [1] of cold electrolytic polishing at a temperature of -50 °C, followed by repeated chemical etching with an appropriate reagent, allows an examination to be made of: (i) the quenched structure before any transformation takes place; (ii) the first sites of discontinuous transformation; (iii) the early stages of growth in the transformed areas.

The above method also enables detection of a second discontinuous transformation (with a 'puzzle' shape) and gives rise to a better quantitative understanding of the boundary displacement rate.

Results

Structural hardening of lead–calcium alloys

Alloys of low calcium content

The ageing mechanism of lead–calcium supersaturated alloys belongs to the family of phase transformations known as 'discontinuous transformations' [2–9]. The detailed hardening mechanism below 100 °C is, however, complex. Some confusion arises with regard to the terminology for this type of phase transformation and the number of successive steps involved in the process. This stems from a wide diversity in the calcium and impurity contents of the alloys, the techniques used to study the alloys, the rates of cooling, the use of as-cast or rehomogenised samples, the possible precipitation of Pb_3Ca, etc.

With lead–calcium alloys, three successive discontinuous reactions are observed in the hardening process. For alloy 786 (Pb–0.58wt.%Ca), the initial hardness of the different states (as-cast cooled at 40 °C s^{-1}; rehomogenised/water-quenched; or rehomogenised/air-cooled) is very low (Fig. 1), i.e., of the order of that of pure lead (5 HV). *The initial discontinuous transformation proceeds in two stages. This has not been observed previously.* The first stage induces a hardening of up to 9 HV for 30 min; the second then starts and lasts for 24 h (12 HV). After 48 h at low temperature, a third reaction begins that induces an initial and slight hardening effect (up to 13 HV) and then an over-ageing after 20 days.

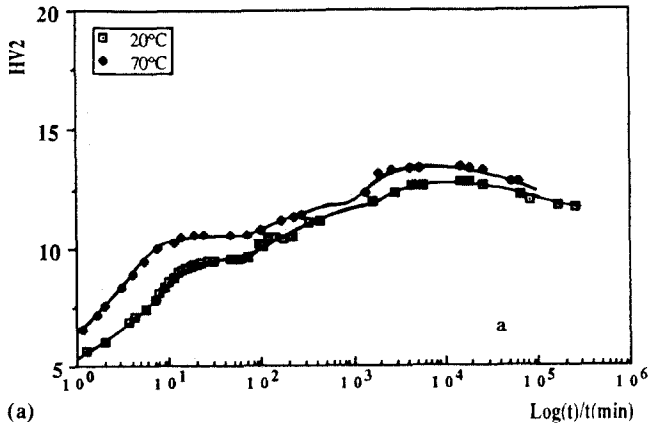

(a)

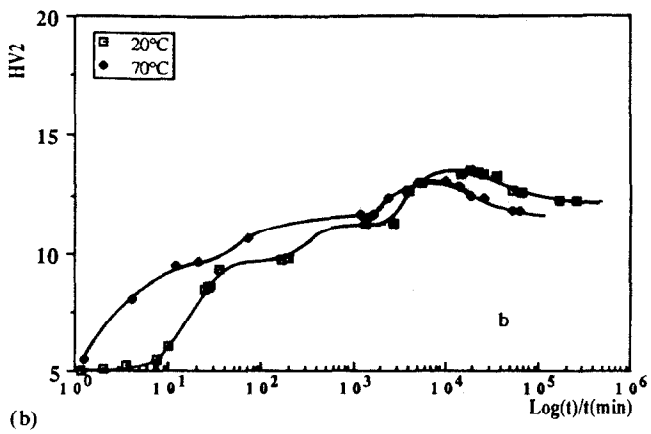

(b)

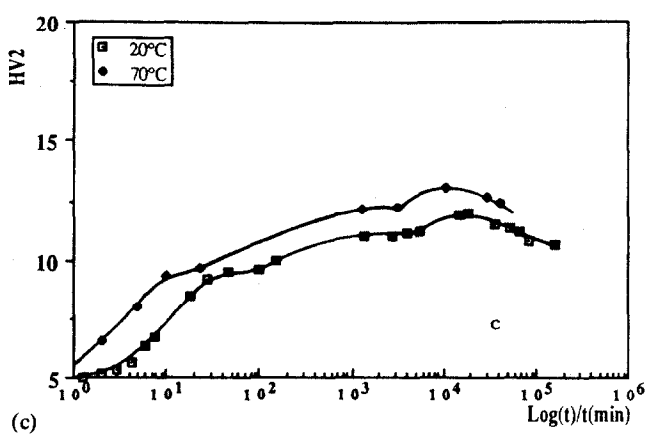

(c)

Fig. 1. Alloy 786 (Pb–0.058wt.%Ca). Hardness evolution vs. time at 20 and 70 °C: (a) as-cast; (b) rehomogenised/water-quenched; (c) rehomogenised/air-cooled.

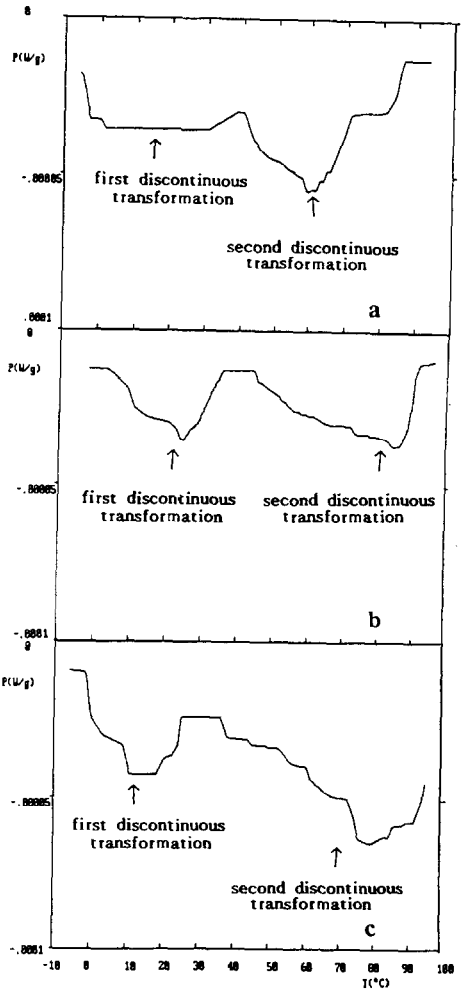

Fig. 2. Alloy 786 (Pb–0.058wt.%Ca). Thermograms obtained at low temperature with a 0.5 °C min^{-1} heating rate: (a) as-cast; (b) rehomogenised/water-quenched; (c) rehomogenised/air-cooled.

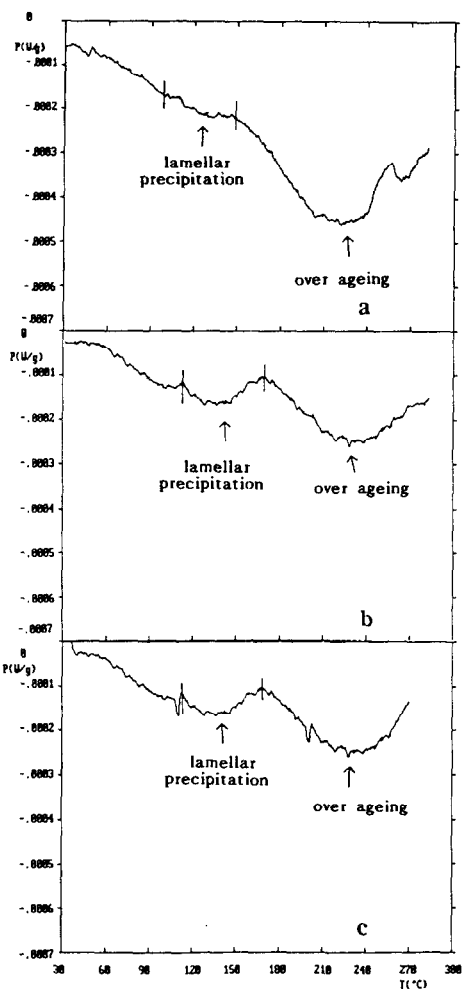

Fig. 3. Alloy 786 (Pb–0.058wt.%Ca). Thermograms obtained at high temperature with a 1 °C min^{-1} heating rate: (a) as-cast; (b) rehomogenised/water-quenched; (c) rehomogenised/air-cooled.

The above three discontinuous transformations of the matrix are also detected by anisothermal calorimetry (Figs. 2 and 3). The thermograms display two easily distinguished exothermic peaks in the temperature range −7 to 95 °C (Fig. 2). The first peak is due to the first discontinuous transformation and is located between −7 and 40 °C. The maximum power dissipation is of the order of 4×10^{-5} W g^{-1} and the energy dissipated in this interval is of the order of 0.20 ± 0.05 J g^{-1}. The second peak, which is located between

40 and 95 °C, corresponds to a second discontinuous reaction that gives grain boundaries with a 'puzzle' shape. The dissipated energy of the second peak is of the order of 0.25 ± 0.05 J g^{-1} with a maximum power of 5×10^{-5} Wg^{-1}. In the range 120 to 285 °C, the thermograms exhibit two exothermic peaks (Fig. 3). The first is due to a third transformation (lamellar discontinuous precipitation with an energy of 0.70 ± 0.7 J g^{-1}). The second corresponds to a mechanism of coalescence and then redissolution (over-ageing).

It is also possible to observe these three transformations of the matrix at room temperature by optical micrography using electrolytic polishing at −50 °C and then a series of chemical attacks of the sample at various times of the ageing process (Figs. 4–6). The study confirms that the sample has not undergone any partial transformation on cooling. During the first transformation, the front of the reaction in each grain is rectilinear and moves at a high rate, viz., 3 to 10 μm min^{-1}. All of the volume of the sample is transformed. The second discontinuous transformation starts about 30 min later at the initial position of the boundary. During the second transformation, the front of the reaction becomes very irregular, like a jigsaw puzzle, and moves at a slow rate, i.e., about 1 μm min^{-1}. This second reaction remains incomplete and does not involve the whole grain. *These two discontinuous reactions take place without precipitation.* About one month after these reactions, a third discontinuous reaction commences in the vicinity of the grain boundaries. This generates thin zones of lamellar precipitation of the Pb_3Ca compound. These observations are qualitatively in good agreement with hardness and calorimetric measurements. For a mean size of 300 μm, and with a rate of 3 to 10 μm min^{-1}, the volumes will be completely transformed within 30 min and lead to a hardness of 9 HV. The second hardening to 11 HV

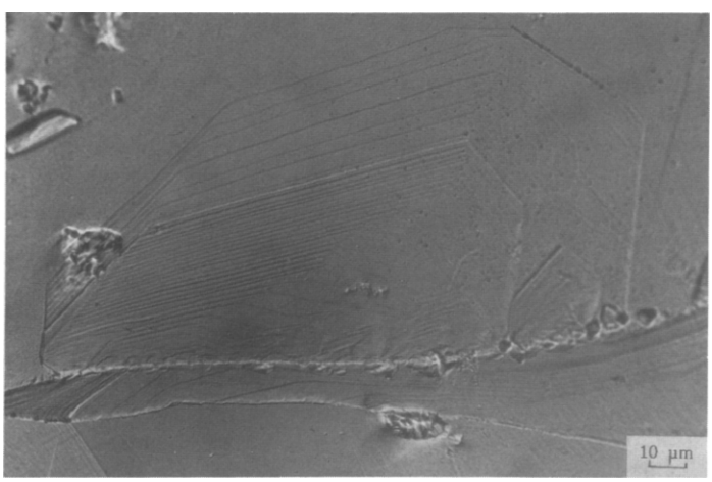

Fig. 4. Alloy 787 (Pb–0.055wt.%Ca–0.007wt.%Ag). Appearance of first discontinuous transformation (regular displacement of the reaction front, apparent rate of boundary movement 1.5 μm min^{-1}) (31 chemical etchings with $\Delta t = 1$ min + 6 chemical etchings with $\Delta t = 6$ min).

Fig. 5. Alloy 793 (Pb–0.093wt.%Ca). First and second discontinuous transformations. Apparent rate of boundary movement: 10 μm and 1 μm min^{-1} for first and second transformations, respectively. 16 etchings with $\Delta t = 2$ min.

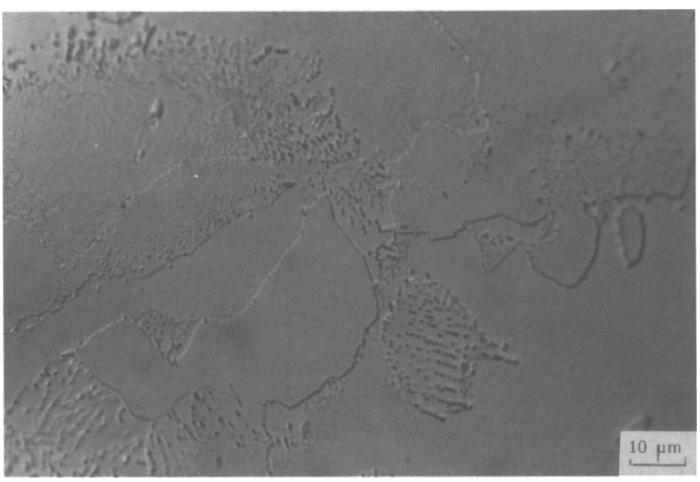

Fig. 6. Alloy 793 (Pb–0.093%Ca). Third discontinuous transformation (incomplete lamellar precipitation of Pb_3Ca). Ageing 52 days at 70 °C.

results from the second discontinuous transformation; the latter transforms only part of the volume.

Influence of calcium content

In the binary lead–calcium alloys, the concentration of calcium determines the quenching ability of the material. For alloys with low calcium content ($\leqslant 0.06$ wt.%), it is quite possible by air-cooling to quench the over-saturated matrix. *The transformation kinetics are very slow and the value*

of the initial hardness corresponds to the beginning of the discontinuous transformation. The latter is influenced neither by the cooling rate nor by the presence of segregation cells in the sample.

For high calcium contents (e.g., 0.09 wt.%), water quenching is necessary to prevent any hardening during cooling. In contrast to rehomogenised alloys, the cellular segregation sub-structure obtained by casting, accelerates the kinetics of all the hardening process. The kinetics of transformation are considerably faster than those for alloys with a low calcium content: the calorimetric peaks characteristic of ageing are displaced towards lower temperatures. Alloy 793 (Pb–0.093wt.%Ca) exhibit peaks at about 10 °C (first discontinuous transformation), 27 °C (second discontinuous transformation), and 94 °C (third discontinuous transformation). The maximum power dissipation is high (i.e., 8×10^{-5} W g^{-1}). The energy dissipated during the first transformation is low. After air cooling, no phenomena are detected during the first transformation reaction. Indeed, the hardness curves show *that the first stage is completed by the end of water cooling (HV = 9).*

Optical micrography shows that at $t = 0$ (i.e., just after quenching) many parts of the grains are already transformed (position of the first front). The rate of movement of the front for the first transformation is 5 to 30 μm min^{-1}, whereas the second transformation is slow (0.1 to 1 μm min^{-1}) and involves only part of the volume. The alloys reach a final hardness of 16 HV.

Influence of Ag, Bi and Al impurities on hardening of lead–calcium alloys

For the different alloys of composition given in Table 1, an investigation has been made of the variation in hardness with time and temperature. This data has been obtained for as-cast, rehomogenised/water-quenched, and rehomogenised/air-cooled samples. Calorimetric analysis and microscopic observations have also been undertaken [10].

In the presence of silver, bismuth or aluminium, the lead–calcium alloys *always harden in three steps.* The hardening mechanisms are analogous to those of the binary lead–calcium alloys. For the same calcium content, there is no additional hardening but the *kinetics of the transformation are not the same.*

Ag (0.001 to 0.007 wt.%) reduces the rate of the discontinuous reaction: the calorimetric peaks are displaced towards higher temperature. The maximum power and the energy dissipated are the same. The apparent rate of the grain-boundary movement during the first discontinuous transformation is low (0.2 to 4 μm min^{-1}). The second transformation is delayed. The alloys do not undergo partial transformation during cooling.

Bi (0.03 to 0.04 wt.%) accelerates the rate of the discontinuous reaction. The calorimetric peaks are displaced towards lower temperatures. The alloys exhibit partial transformation during cooling. The apparent rate of the grain-boundary movement is high.

With Al (0.01 to 0.08 wt.%), a refining of the grains is observed: the diameter of the grains is reduced and the number of transformation sites is increased. In addition, the rate of the grain-boundary movement is decreased, but, in general, the kinetics of the first transformation are accelerated.

Kinetics of transformation

Decomposition of the supersaturated matrix by heating is complex: three discontinuous transformations, are involved. For each mechanism, we have assumed that the transformed volume can be represented by a mathematical law and that the isothermal kinetics are independent. Many reactions obey the relationship:

$$v = \frac{dx}{dt} = n\,k^n\,t^{n-1}\,(1-x) \tag{1}$$

This reduces to the Johnson–Mehl law:

$$x = 1 - \exp - (k\,t)^n \tag{2}$$

(where x = volume transformed in time t).

Considering the experimental curves HV $= f(t)$, for the first discontinuous transformation we can write:

$$x = \frac{\text{HV} - \text{HV (initial)}}{\text{HV (final)} - \text{HV (initial)}} = f(t) \tag{3}$$

Figure 7 shows x versus time at 20, 52 and 70 °C for the alloy 786 (Pb–0.058wt.%Ca), and Fig. 8 ln ($-$ ln $(1-x)$) versus ln (t). The latter yields parallel straight lines of slope n.

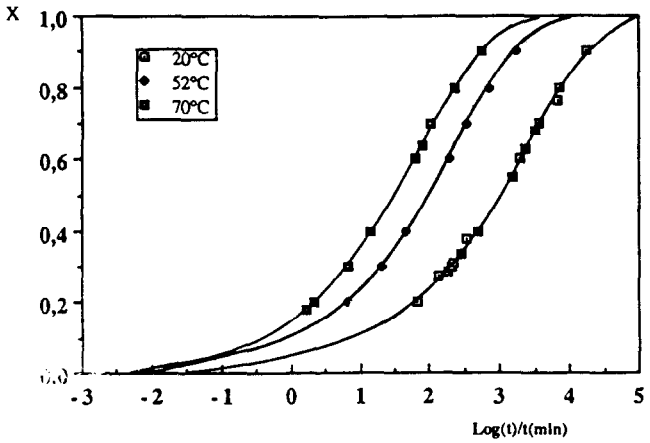

Fig. 7. Alloy 786 (Pb–0.058wt.%Ca). Parameter x as a function of time (t) (see text) at 20, 52 and 70 °C for the first discontinuous transformation. HV (initial) = 5.

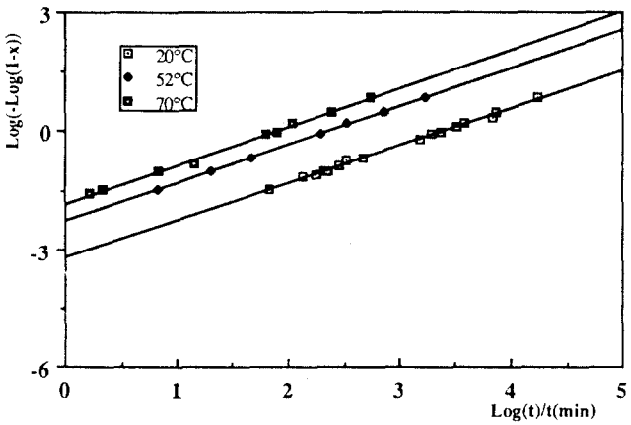

Fig. 8. Alloy 786 (Pb–0.058wt.%Ca). ln $(-\ln(1-x))$ vs. ln (t) at 20, 52 and 70 °C for first discontinuous transformation.

Christian [11] distinguishes two mechanisms: one controlled by the interface, the other by a volume diffusion process. A value of $n = 1$ corresponds to the former mechanism. Germination is located at the grain boundaries. The kinetics of germination are equal to zero at the beginning of the transformation. Cahn [12] considers that the Johnson–Mehl with $n = 1$ holds when the initial rate of germination is very high. Under this condition, saturation is reached immediately before the growth. This mechanism corresponds precisely with our microscopic observations.

The activation energy, Q, can be calculated from the variation of k with temperature, i.e., the Arrhenius law:

$$k = k_0 \exp(-Q/RT) \tag{4}$$

Figure 9 gives a plot of $\ln k$ versus $1/T$. From this, a value of $Q = 11.2$ kJ mol^{-1} is obtained. The activation energy does not depend on the parameter x. The value for Q was also obtained by the method of Burke [13]. The latter involves measuring the time required to reach x. Plots of $\log t_x$ versus $1/T$ for different values of x yields $11.2 < Q < 11.6$ kJ mol^{-1}. When the second and third transformations are involved, it is difficult to resolve the kinetic law.

With alloy 793 (Pb–0.093wt.%Ca), when rehomogenised and air-cooled, it is possible to determine the kinetic law for the third discontinuous precipitation. Using eqns. (2) and (3), a value of $n = 1$ and an activation energy of 69 kJ mol^{-1} are obtained. The apparent rate of movement of the boundaries can be measured directly on the polished sample after heat treatment and etching. Figure 10 shows the same grain after heat treatment at 72, 20 and -5 °C. Figure 11 gives the dependence of $\ln v$ on $1/T$ for the alloy 765. The energy of activation is $13.2 < Q < 21.4$ kJ mol^{-1}.

The kinetics are modified in the presence of Ag, Bi and Al impurities. For high levels of Ca, or with Bi impurity, the first transformation com-

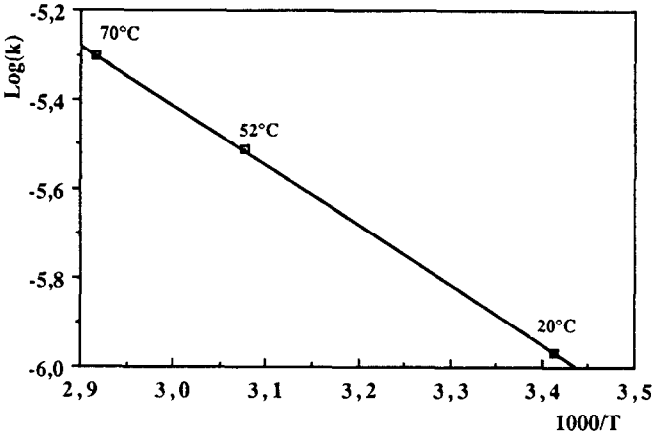

Fig. 9. Alloy 786 (Pb–0.058wt.%Ca). Determination of activation energy for first discontinuous transformation.

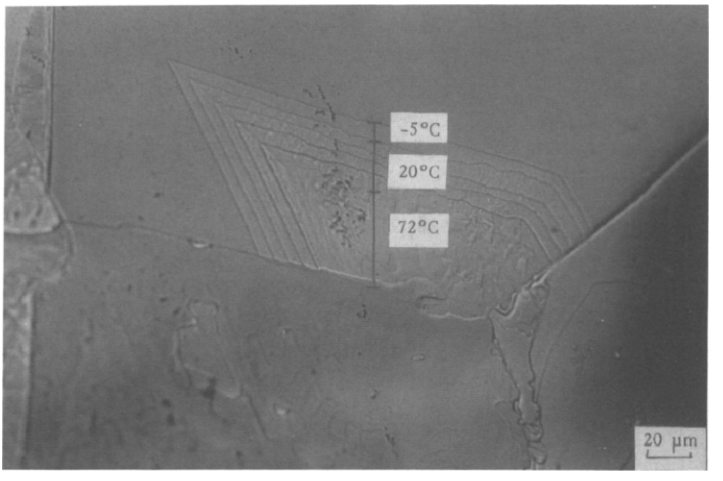

Fig. 10. Alloy 765 (Pb–0.044wt.%Ca–0.0312wt.%Bi). Determination of grain boundary movement rate for first discontinuous transformation: 72 °C: etching 3 times, all 10 min; 20 °C: etching 4 times, all 10 min; −5 °C: etching once, 20 min.

mences during cooling. Thus, it is not possible to determine a mathematical kinetic law.

Table 2 summarizes the results obtained with the different alloys.

Structural hardening of lead–calcium–tin alloys

Background

There have been many studies of lead–calcium–tin alloys [7, 14–19]. According to Borchers and Assmann [14, 15] and Prengaman [16, 17], these

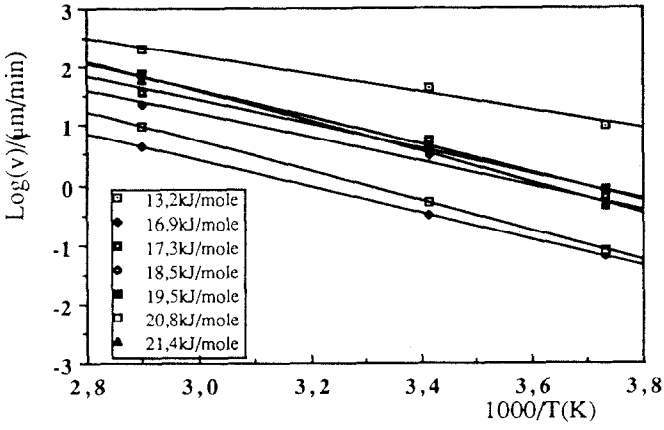

Fig. 11. Alloy 765 (Pb–0.044wt.%Ca–0.0312wt.%Bi). Determination of the activation energy for first discontinuous transformation.

ternary alloys are characterised by the ratio $r = \mathrm{Sn/Ca}$. For high r values, hardening occurs after an incubation period and proceeds via continuous micro-precipitation of intermetallic compound. Views differ as to whether the phases present in the alloy are relatively pure Pb_3Ca and Sn_3Ca or $(PbSn)_3Ca$. The limits of the solubility of Ca and Sn in Pb at 20 °C are uncertain [2, 7, 16, 20–24]. The difference between the hardening of as-cast samples and rehomogenised samples is not known. We have determined the enthalpy of formation of Sn_3Ca and Pb_3Ca to be -38.6 ± 0.8 and -34.0 ± 0.5 kJ(mol atom)$^{-1}$, respectively, with reference to solid metals [25–27] at 300 K. These data show that Sn_3Ca is more stable than Pb_3Ca.

We have prepared one series of alloys with a constant content of Ca (0.11 wt.%) but a variable content of Sn (0.24 to 1.09 wt.%), and a second series with a constant ratio of Sn/Ca (≈ 3 atomic) and variable Sn and Ca contents (Table 1). As before, these alloys have been examined in three states (viz., as-cast, rehomogenised/water-quenched, rehomogenised/air-cooled).

Hardening of alloys having variable Sn/Ca ratio

Four alloys with increasing Sn/Ca ratio have been studied: 748 ($r = 0.67$); 776 ($r = 1.24$), 779 ($r = 1.96$); 780($r = 3.35$). The results obtained with alloy 748 are discussed here.

Figure 12 shows the change in hardness with time at 20, 52, 67 and 85 °C for the as-cast sample. The initial hardness is 10.5 HV. The hardening process appears to be very fast; it commences during cooling and continues immediately after quenching, as was found for binary lead–calcium alloys (*first discontinuous transformation*). *The second discontinuous transformation is very slow and incomplete.* After an incubation period of 10 days, the hardness increases and reaches 15 HV after one year at 20 °C. The incubation period decreases with increase in temperature (Fig. 13). *The third transformation*

TABLE 2

Kinetics of transformation

Alloy	State	Temperature (°C)	n	k (s^{-1})	Activation energy Q (kJ mol^{-1})
786		20	1.00	2.56×10^{-3}	11.2
First discontinuous	as-cast	52	0.99	4.04×10^{-3}	
transformation		70	0.99	4.99×10^{-3}	$11.2 < Q < 11.5$
793		20	0.99	3.90×10^{-7}	69
Third discontinuous transformation	air-cooled	70	0.99	2.44×10^{-5}	
787		20	0.95	5.65×10^{-4}	
First discontinuous	as-cast	52	0.97	1.56×10^{-3}	25
transformation		70	0.97	2.50×10^{-3}	$24.9 < Q < 25.3$
783		20	1.00	2.26×10^{-7}	
Third discontinuous transformation	air-cooled	70	1.00	2.20×10^{-5}	76
777					
First discontinuous transformation	as-cast	20	1.00	4.35×10^{-3}	
778		20	1.05	2.88×10^{-7}	
Third transformation	air-cooled	70	1.04	6.82×10^{-6}	53
			v (μm min^{-1})		
765		−5	0.16 to 2.67		
First discontinuous	as-cast	20	0.76 to 5.17		$13.2 < Q < 21.4$
transformation		72	1.9 to 10.00		

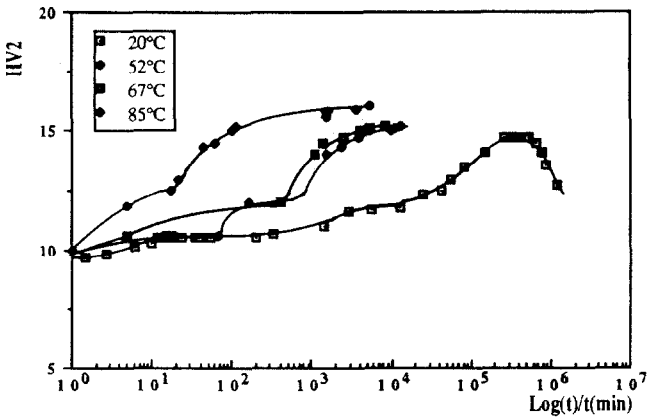

Fig. 12. Alloy 748 (Pb–0.12wt.%Ca–0.24wt.%Sn). Hardness evolution at 20, 52, 67 and 85 °C. As-cast sample.

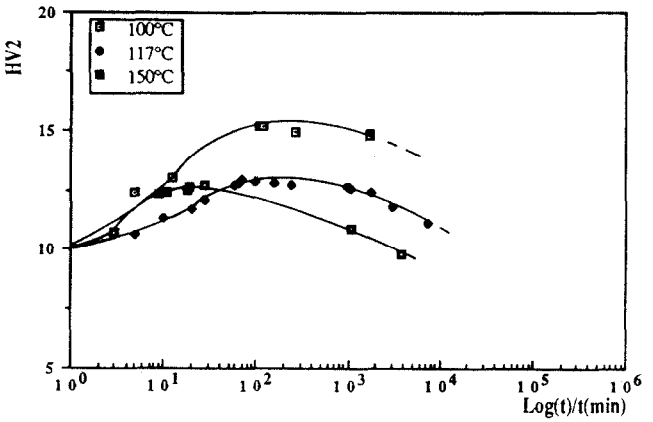

Fig. 13. Alloy 748 (Pb–0.12wt.%Ca–0.24wt.%Sn). Hardness evolution at 100, 117 and 150 °C. As-cast sample.

corresponds to an homogeneous precipitation of intermetallic compound. After a very long time, the hardness is found to decrease. This corresponds to a *fourth discontinuous precipitation* (*over-ageing*).

Figure 14 gives values for the hardness at 20 °C for the three states: as-cast, rehomogenised/water-quenched, rehomogenised/air-cooled. After rehomogenising and water quenching, the initial hardness is very low (5 HV) and about the same as that for pure lead. This confirms that the cellular structure caused by calcium and tin segregation during solidification in the as-cast samples accelerates the kinetics of the first discontinuous transformation and decreases the incubation period of the third continuous transformation (Fig. 14).

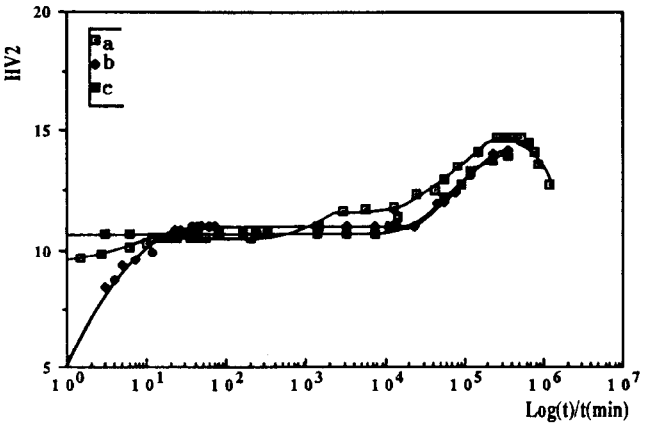

Fig. 14. Alloy 748 (Pb–0.12wt.%Ca–0.24wt.%Sn). Hardness evolution at 20 °C: (a) as-cast sample; (b) rehomogenised/water-quenched; (c) rehomogenised/air-cooled.

Microscopic studies of samples after cooling confirms that the first discontinuous transformation is almost achieved in the as-cast samples. The rate of boundary movement in the second discontinuous transformation is very small, viz., 0.1 to 1 μm min^{-1}. After rehomogenising and water quenching, the structure is equiaxial. Boundary movement during the first transformation is about 1 to 3 μm min^{-1} and decreases with time. This is contrary to that found with binary lead–calcium alloys. We attribute this behaviour to the germination of the intermetallic compound of the third continuous transformation.

Figure 15 shows that precipitates after 1 h at 89 °C. The diffraction patterns of Pb and $(PbSn)_3Ca$ are given in Fig. 16. The parameters for Pb, Pb_3Ca, Sn_3Ca are almost the same, i.e., 4.9506, 4.901 and 4.742 Å, respectively.

Thermograms (Fig. 17) exhibit two exothermic peaks in the temperature range −10 to 70 °C. The first peak, due to the first discontinuous transformation, is absent for both the as-cast and the rehomogenised/air-cooled samples.

In the presence of tin, the second discontinuous transformation is very incomplete. The maximum power dissipation is about 5×10^{-5} W g^{-1} while the energy dissipated in the range −7 to +70 °C is about 0.23 ± 0.02 J g^{-1}. These values are greater with binary lead–calcium alloys with the same calcium content. The third continuous precipitation commences at about 70 °C. At a heating rate of 1 °C min^{-1}, the maximum power of the third transformation is of the order of 1.6×10^{-4} W g^{-1} at 120 °C for the as-cast sample, or at 140 °C for the rehomogenised sample. The energy dissipated between 90 and 160 °C is 0.41 ± 0.04 J g^{-1} (Fig. 18).

The fourth discontinuous transformation $[\alpha + (PbSn)_3Ca \rightarrow \alpha + (PbSn)_3Ca]$ is not perceptible with alloy 748 but can be detected in alloys 776 and 780.

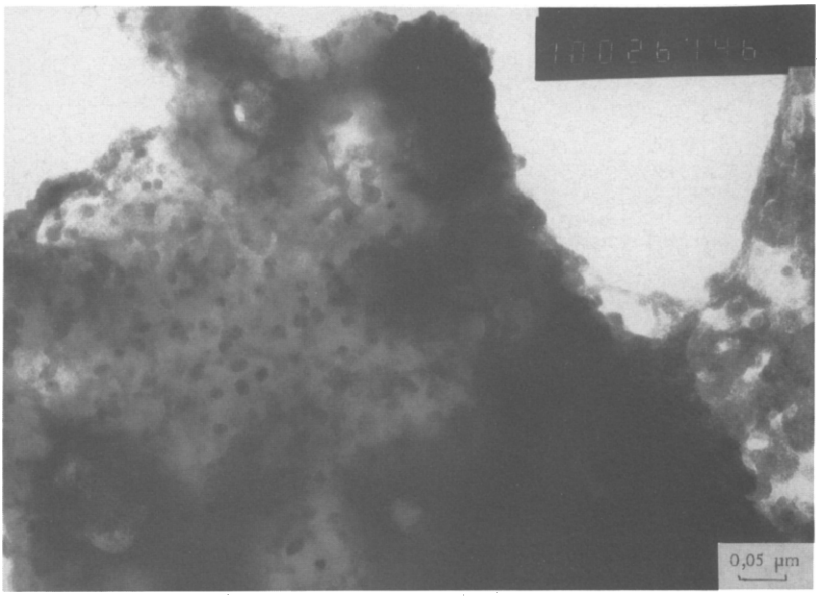

Fig. 15. Alloy 748 (Pb–0.12wt.%Ca–0.24wt.%Sn). Precipitation of $(PbSn)_3Ca$ after 1 h at 89 °C.

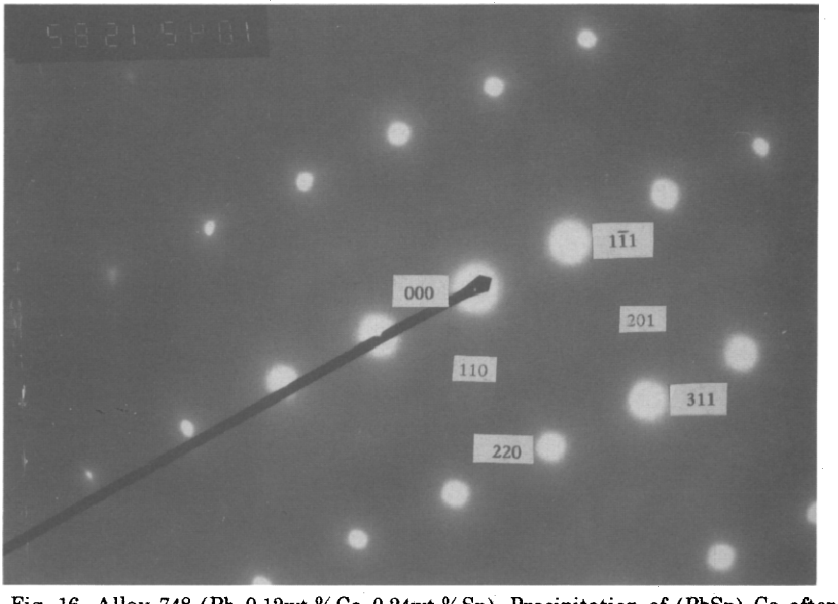

Fig. 16. Alloy 748 (Pb–0.12wt.%Ca–0.24wt.%Sn). Precipitation of $(PbSn)_3Ca$ after 1 h at 89 °C. Micro-diffraction patterns and spots of the matrix Pb and intermetallic compound $(PbSn)_3Ca$.

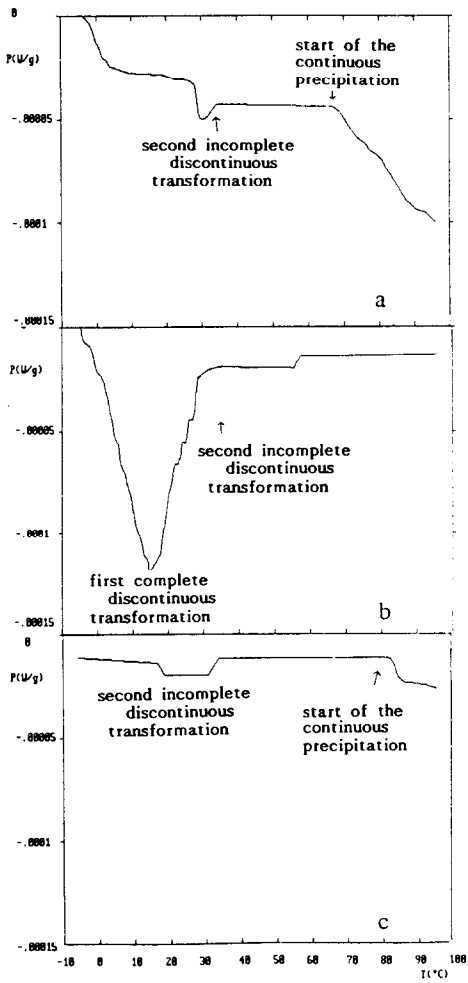

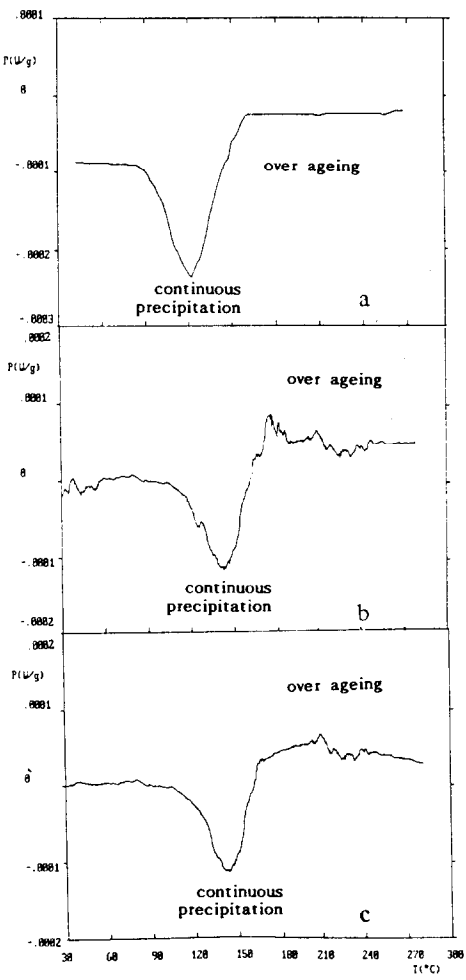

Fig. 17. Alloy 748 (Pb–0.12wt.%Ca–0.24wt.%Sn). Thermograms obtained at low temperature with 0.5 °C min^{-1} heating rate: (a) as-cast; (b) rehomogenised/water-quenched; (c) rehomogenised/air-cooled.

Fig. 18. Alloy 748 (Pb–0.12wt.%Ca–0.24wt.%Sn). Thermograms obtained at high temperature with 1 °C min^{-1} heating rate: (a) as-cast; (b) rehomogenised/water-quenched; (c) rehomogenised/air-cooled.

With a higher Sn/Ca ratio, the over-ageing (fourth discontinuous lamellar transformation) is accelerated. Figure 19 presents the lamellar precipitation obtained after 40 days at 100 °C with alloy 776 (Pb–0.12wt.%Ca–0.14wt.%Sn). The dispersive energy spectrum (Fig. 20) confirms the simultaneous presence of Ca, Sn and Pb. It is not known whether the Pb originates from the matrix or from the precipitate.

With increasing Sn/Ca ratio, the initial rate of boundary movement decreases. Both the maximum exothermic power and the energy associated

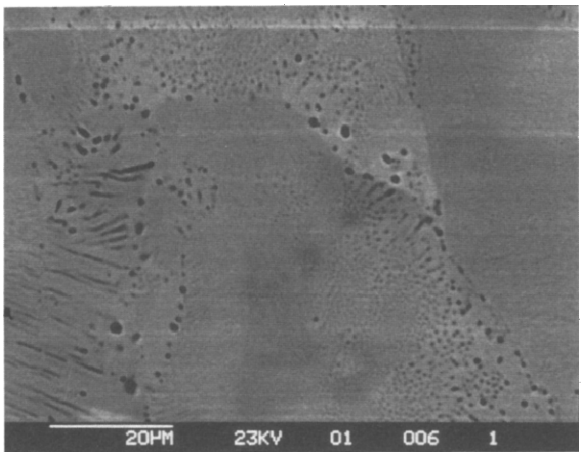

Fig. 19. Alloy 776 (Pb–0.12wt.%Ca–0.44wt.%Sn). Fourth discontinuous transformation with increase in size of precipitates and decrease in hardness (over-ageing) after heating at 100 °C for 40 days.

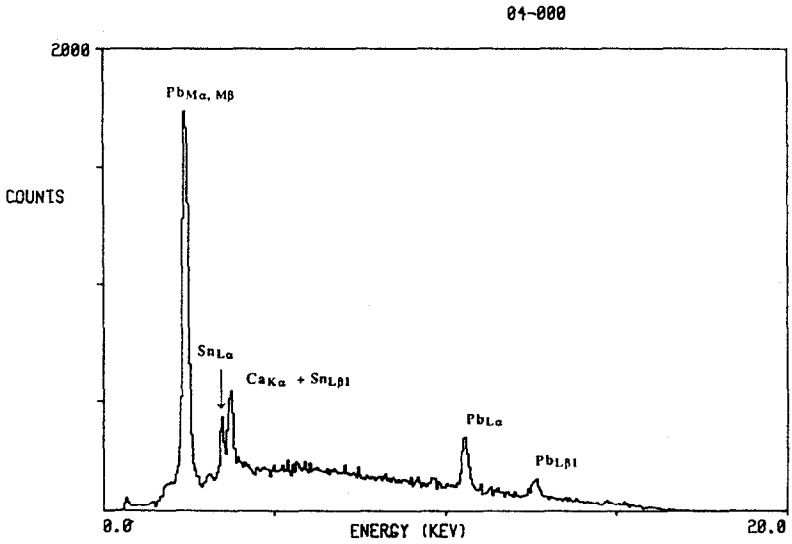

Fig. 20. Alloy 776 (Pb–0.12wt.%Ca–0.44wt.%Sn). Heating 40 days at 100 °C. Presence of Sn, Ca and Pb in precipitate.

with the first discontinuous transformation are slower. There is no second transformation. By contrast, the third continuous precipitation is accelerated: the calorimetric peak is displaced towards lower temperatures (107 °C for alloy 776).

Figure 21 presents the hardness evolution versus time and temperature for alloy 780 (Pb–0.11wt.%Ca–1.09wt.%Sn). Pre-precipitation of $(PbSn)_3Ca$ during the third continuous transformation involves an initial hardness of

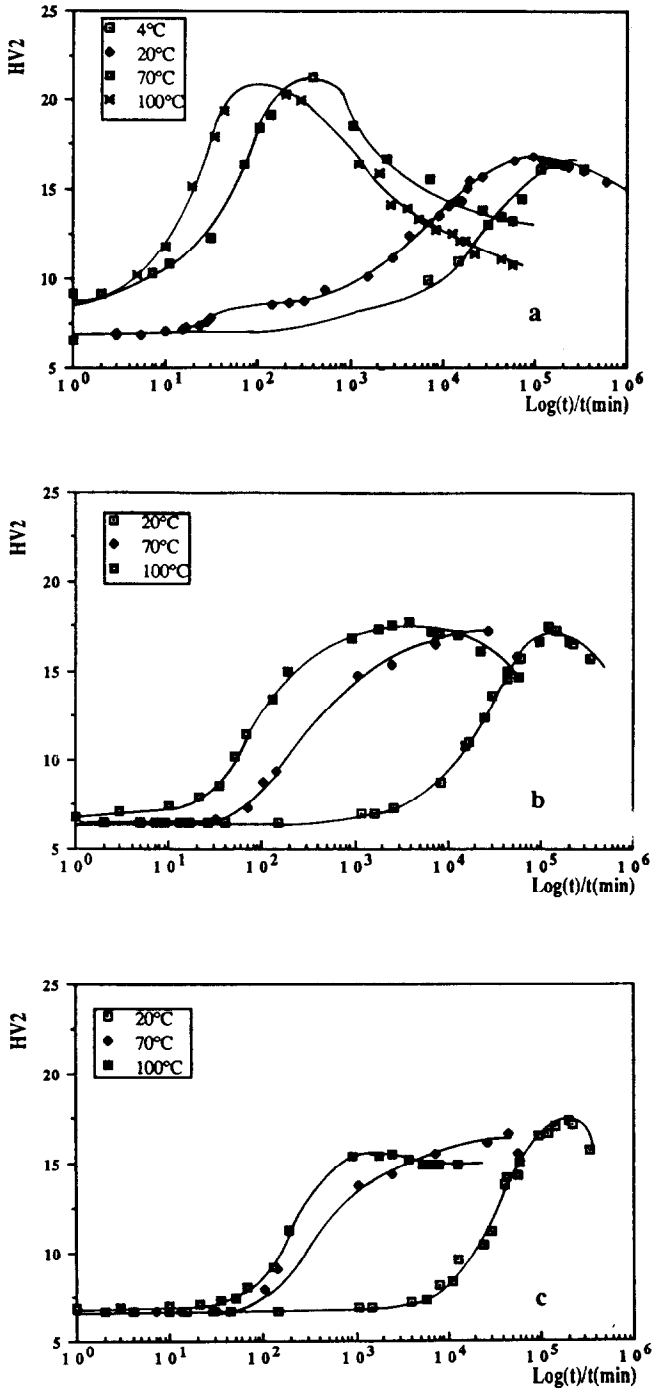

Fig. 21. Alloy 780 (Pb–0.11wt.%Ca–1.09wt.%Sn). Hardness evolution at 20, 70 and 100 °C: (a) as-cast; (b) rehomogenised/water-quenched; (c) rehomogenised/air-cooled.

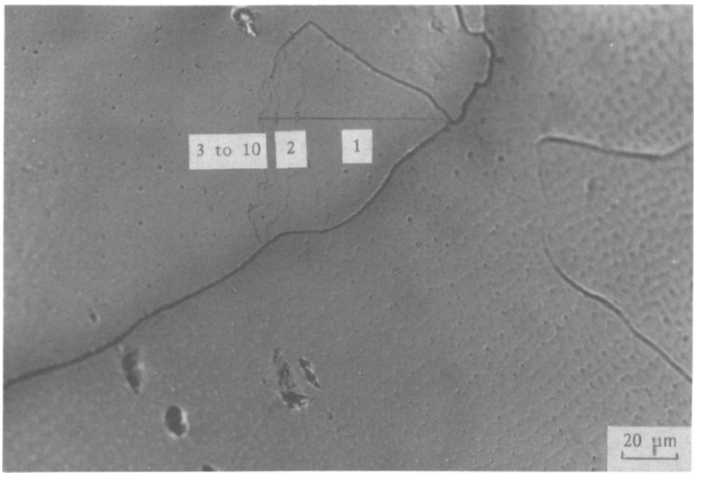

Fig. 22. Alloy 780 (Pb–0.11wt.%Ca–1.09wt.%Sn). First discontinuous transformation. Periodic chemical attacks after heating at 100 °C (10 times $\Delta t = 5$ min). Decrease of rate of boundary movement with time.

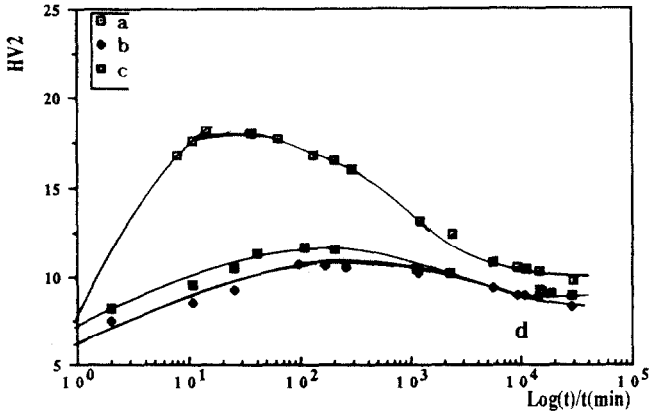

Fig. 23. Alloy 780 (Pb–0.11wt.%Ca–1.09wt.%Sn). Hardness evolution at 150 °C: (a) as-cast; (b) rehomogenised/water-quenched; (c) rehomogenised/air-cooled.

7 HV. This reduces the over-saturation and restrains boundary movement during the first discontinuous transformation.

With the as-cast sample, the first transformation exists but is extremely incomplete. This is a new observation. The transformation is absent for rehomogenised samples. The final hardness does not depend on the cooling rates.

The rate of boundary movement for the as-cast sample is very slow. It is initially 4×10^{-3} µm min^{-1} and then reaches 0.1×10^{-3} µm min^{-1} (Fig. 22). The rate increases with temperature.

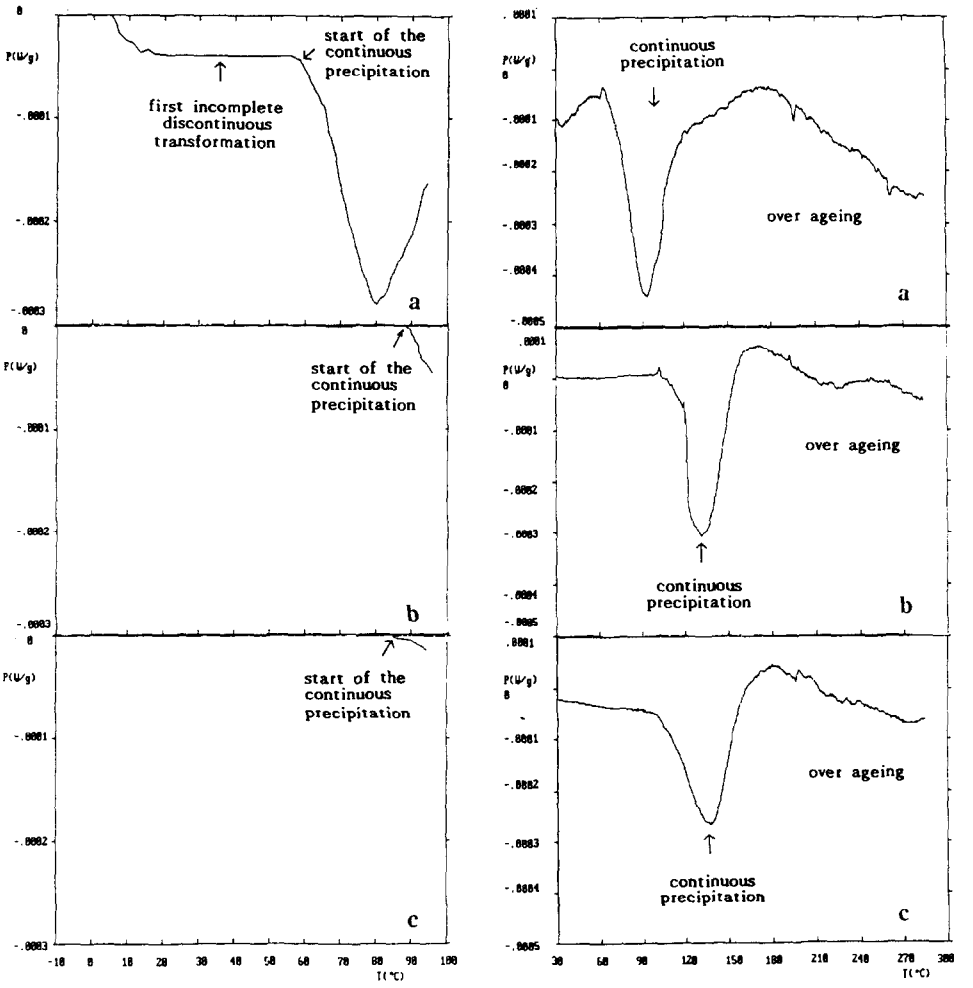

Fig. 24. Alloy 780 (Pb–0.11wt.%Ca–1.09wt.%Sn). Thermograms obtained at low temperature, with 0.5 °C min^{-1} heating rate: (a) as-cast; (b) rehomogenised/water-quenched; (c) rehomogenised/air-cooled.

Fig. 25. Alloy 780 (Pb–0.11wt.%Ca–1.09wt.%Sn). Thermograms obtained at high temperature, with 1 °C min^{-1} heating rate: (a) as-cast; (b) rehomogenised/water-quenched; (c) rehomogenised/air-cooled.

The incubation period for the third continuous transformation is longer for rehomogenised samples (48 h) than for as-cast samples (24 h). The cellular segregation structure delays the fourth discontinuous transformation (over-ageing) and decreases the hardness (Figs. 21 and 23). Data obtained using anisothermal calorimetry (Figs. 24 and 25) show essentially the peaks of the third continuous precipitation and the fourth discontinuous precipitation. The first discontinuous transformation is hardly visible with as-cast samples.

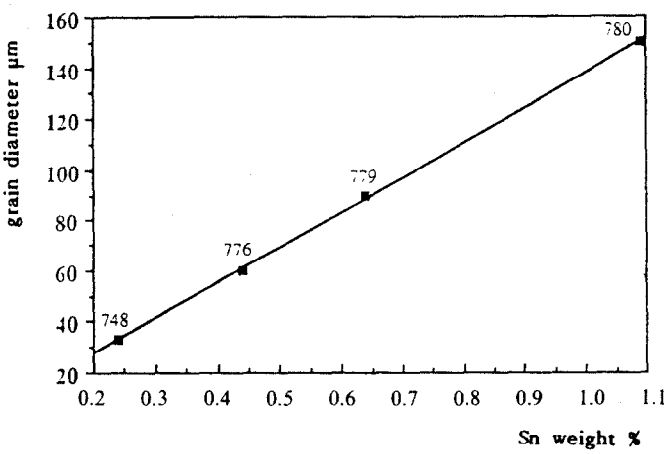

Fig. 26. Grain diameter as a function of Sn content (X) in Pb–0.12wt.%Ca–X%Sn alloy.

The maximum power and the energy dissipated during the third transformation becomes larger with increase in tin content for a constant calcium content. For an increase in tin content from 0.24 to 1.09 wt.%, the maximum power increases from 1.6×10^{-4} to 4.39×10^{-4} W g^{-1}, and the energy dissipated from 0.41 to 1.2 J g^{-1}. The diameter of the grains also increases with tin content (Fig. 26).

Hardening of alloys having constant Sn/Ca ratio (r = 3)

Development of the hardness of the alloys 771, 766, 767 with time and temperature, as well as calorimetric results, are the same as those for alloy 780. In all cases, the first discontinuous transformation exists only with the as-cast samples, but is very incomplete. The second discontinuous transformation is absent. The incubation period of the third continuous precipitation is shorter with as-cast samples than with rehomogenised samples.

The exothermic energy ΔH dissipated during the third continuous precipitation is equal to 52 ± 5, 58 ± 6, 59 ± 6 and 48 ± 5 kJ per mole $(PbSn)_3Ca$ for the alloys 767, 766, 771 and 780, respectively. Thus, on average, a value of -54 ± 5 kJ mol^{-1} or -14 ± 1 kJ(mol atom)$^{-1}$ is obtained. We must modify this value for the enthalpy of dissolution of solid Ca and solid Sn in solid Pb in order to obtain the enthalpy of formation of $(PbSn)_3Ca$. The dissolution enthalpy of solid Sn in solid Pb is $\Delta H(Sn) = 15.98$ kJ mol^{-1} [28]. The enthalpy of dissolution of solid Ca in solid Pb is estimated to be $4\Delta G_f(Pb_3Ca)$. According to Notin *et al.* [27], $\Delta G_f(Pb_3Ca) = -32.86$ kJ mol^{-1} at 300 K. Thus, $\Delta H(Ca) = -131.44$ kJ mol^{-1}. If the precipitate is Sn_3Ca, then $\Delta H_f(Sn_3Ca) = \Delta H + \Delta H(Ca)/4 + 3\ (\Delta HSn)/4 = -34.87$ kJ(mol atom)$^{-1}$; *cf.*, -38.6 ± 0.8 kJ(mol atom)$^{-1}$ at 300 K [25–27].

Influence of impurities Ag, Bi and Al

For the alloys 780, 781, 749, 782 and 792 (Table 1), plots have been made of the variation of hardness with time and temperature. Calorimetric analysis

and microscopic observations have also been conducted [10]. With Ag, for $r = 3$, an increase is observed in the rate of continuous $(PbSn)_3Ca$ micro-precipitation. In addition, the incubation time is reduced. For $r = 1.3$, a delay occurs in the discontinuous transformation. By contrast, Al and Bi accelerate slightly the continuous precipitation.

Conclusions

The ageing mechanism of lead–calcium supersaturated alloys proceeds via a number of steps. Three discontinuous reactions have been detected using the techniques of anisothermal calorimetry, hardness measurement and optical microscopy.

During the first transformation, all of the volume of the sample is transformed through movement of the different boundaries. The rate of movement is about 3 to 10 $\mu m\ min^{-1}$. The transformation induces a hardening of up to 9 HV. The thermograms exhibit an exothermic peak between -7 and 40 °C, with a maximum power of $4 \times 10^{-5}\ W\ g^{-1}$ and a dissipated energy of $0.20\ J\ g^{-1}$.

The second transformation commences after the first at the initial position of the boundaries. The transformation is incomplete. The front of the reaction is very irregular and moves at a slow rate. The thermograms display an exothermic peak between 40 and 95 °C, with a maximum power of $5 \times 10^{-5}\ W\ g^{-1}$ and an energy of $0.25\ J\ g^{-1}$. This transformation induces a hardening of 12 HV.

The above two discontinuous transformations occur without precipitation. Then, a third reaction begins that induces an initial and slight hardening effect (13 HV) followed by over-ageing. The thermograms show peaks at 140 °C, with an energy of $0.7\ J\ g^{-1}$. This third discontinuous transformation generates thin zones of lamellar precipitates of Pb_3Ca in the vicinity of the grain boundaries.

With high levels of calcium, the transformation kinetics are accelerated and the calorimetic peaks move to lower temperature. Water quenching is required in order to prevent any hardening during cooling.

In the presence of Ag, Bi or Al, the PbCa alloy always hardens in three steps. The hardening mechanisms are analogous. Bi accelerates the transformation, while Ag delays it. A refining of the grains is observed with Al.

The transformed volumes can be represented by the Johnson–Mehl law with a value of $n = 1$. This corresponds to an interfacial control. The energies of activation are all much lower than that for the auto-diffusion of Pb.

In lead–calcium–tin alloys, the hardening process is influenced by the Sn/Ca ratio, r. For very low values of r, the hardening process is the same as that for lead–calcium alloys. At high values of r ($\geqslant 3$, in atoms) a continuous precipitation of $(PbSn)_3Ca$ is found after an incubation period. Then follows a discontinuous precipitation with increase in the size of the $(PbSn)_3Ca$ (over-ageing). With as-cast samples, however, the first incomplete discontinu-

ous transformation is always detected. With intermediate values of r, four transformations take place in sequence: first discontinous transformation, second discontinuous transformation, third continuous precipitation ($(PbSn)_3Ca$), fourth discontinuous precipitation (increase in size of $(PbSn)_3Ca$).

All the mechanisms are thermally activated. The cellular structure caused by Ca and Sn segregation during solidification also accelerates the kinetics of the transformations.

Each transformation gives a calorimetric peak, but we detect essentially the peak of the third continuous precipitation. The associated energy increases with Sn content at constant Ca content. The value of the enthalpy of formation of $(PbSn)_3Ca$ is close to that for Sn_3Ca.

With lead–calcium–tin alloys, Ag increases the rate of the continuous precipitation and reduces the incubation period. Al and Bi slightly enhance the continuous precipitation.

References

1 J. P. Hilger and A. Boulahrouf, *Mater. Charact., 24* (1990) 159.
2 E. E. Schumacker and G. B. Bouton, *Met. Alloys, 1* (1930) 405.
3 W. Scharfenberger and S. Henkel, *Z. Metallkd., 64* (1973) 478.
4 H. Borchers, W. Scharfenberger and S. Henkel, *Z. Metallkd., 66* (1975) 111.
5 R. D. Prengaman, *Electrochemical Society, Fall Meet., Las Vegas, NV, Oct. 1976.*
6 T. W. Caldwell and U.S. Sokolov, *J. Electrochem. Soc., 123* (1976) 972.
7 D. E. Kelly, *Thesis*, Waterloo University, Canada, 1985.
8 A. Boulahrouf, *Thèse de Doctorat*, Université de Nancy I, France, 1989.
9 J. L. Caillerie, J. Hertz, A. Boulahrouf, M. Dirand and J. P. Hilger, *Proc. 9th Int . Lead Conf., Goslar, F.R.G., Oct. 1986*, Lead Development Association, 1988 p. 57.
10 L. Bouirden, *Thèse d'Etat*, Université de Nancy I, France, 1990.
11 J. W. Christian, *The Theory of Transformation in Metals and Alloys*, Pergamon, Oxford, 1965.
12 J. W. Cahn, *Acta Metall., 4* (1956) 449, 572.
13 J. Burke, *The Kinetics of Phase Transformation in Metals*, Pergamon, Oxford, 1965.
14 H. Borchers and H. Assmann, *Z. Metallkd., 69* (1978) 43.
15 H. Borchers and H. Assmann, *Metallurgia, 33* (1979) 936.
16 R. D. Prengaman, *Electrochemical Society, Fall Meet., Las Vegas, NV, 1980.*
17 R. D. Prengaman, *7th Int. Lead Conf., Madrid, Spain, 1980.*
18 M. Meyers, H. R. Van Handle and C. R. Di Martini, *J. Electrochem. Soc., 121* (1974) 1526.
19 M. Meyers, *Proc. 87th Convention Battery Council Int., Hollywood, FL, 1975*, p. 135.
20 J. Cahn and H. N. Treaftis, *Trans. AIME, 218* (1960) 376.
21 R. Nozato, *Bull. Univ. Osaka Prefect. Ser., 10* (1962) 477.
22 E. Schurmann and F. J. Gilhaus, *Arch. Eisenhüttenwes., 32* (1961) 867.
23 I. Karakaya and W. T. Thomson, *Bull. Alloy Phase Diagrams*, (1987) 144.
24 P. Adeva, G. Caruana, M. Aballe and M. Torralba, *Mater. Sci. Eng., 54* (1982) 229.
25 L. Bouirden, *Thèse de Doctorat de 3ème Cycle*, Université de Nancy I, France, 1984.
26 L. Bouirden, M. Notin and J. Hertz, *Proc. XV Journées de Calorimétrie et d'Analyse Thermique (JACT), Brussels, Belgium, 1984*, p. 309.
27 M. Notin, L. Bouirden, E. Belbacha and J. Hertz, *J. Less-Common Met., 154* (1989) 121.
28 R. Hultgreen, P. D. Desai, D. T. Hawkings, M. Gleiser and K. K. Kelly, *Selected Values of the Thermodynamics Properties of Binary Alloys*, American Society for Metals, Metals Park, OH, 1973.